IEEE Access
Multidisciplinary | Rapid Review | Open Access Journal

Received February 5, 2019, accepted February 21, 2019, date of publication February 25, 2019, date of current version March 12, 2019.

Digital Object Identifier 10.1109/ACCESS.2019.2901440

CP Antenna Array With Switching-Beam Capability Using Electromagnetic Periodic Structures for 5G Applications

MOHAMAD MANTASH, (Senior Member, IEEE), AND TAYEB A. DENIDNI, (Fellow Member, IEEE)
Institut National de la Recherche Scientifique-Energie, Materiaux et Telecommunications, Montreal, QC H5A1K6, Canada
Corresponding author: Mohamad Mantash (mohamad.mantash@emt.inrs.ca)

This work was supported by the Natural Sciences and Engineering Research Council of Canada.

ABSTRACT This paper proposes a novel circularly polarized electromagnetic band-gap (EBG) antenna array backed by an artificial magnetic conductor (AMC) that operates in the 26–32-GHz bands. The designed antenna is a 2×2 Yagi–Uda antenna array that uses the directors' semicircles to direct the radiation in the horizontal end-fire direction. The feeding of the array is designed with two parallel T-junction portions forming a parallel feeding network that converts the polarization from linear to circular. An AMC is placed underneath the antenna to suppress the backward radiation and obtain the propagation only in the $+z$ plane. The novel approach is based on the fact that EBGs are placed around the array to give to the antenna, beam-switching capability. This simple technique provides a high beam tilting angle of $+90^\circ$ from the end-fire to the full broadside plane. The final EBG-AMC-antenna array is circularly polarized and presents, at 29 GHz, a gain of 11.9 dBi, and an axial ratio bandwidth of 10% from 28 to 31 GHz. By assessing the high antenna performances presented in this paper, and the high angle beam-switching capability by adding the EBG, the novel array could be seen as a potential candidate for implementation in future 5G applications.

INDEX TERMS Antenna array, artificial magnetic conductor (AMC), circular polarization, EBG structures, millimeter wave antennas, multi-feeding, periodic structures.

I. INTRODUCTION

Millimeter-wave (MM-wave) circularly-polarized (CP) antennas with planar configuration have attracted numerous researchers because of their robustness, low cost and high radiation efficiency. For some MM-wave applications, such as 5G applications, broadband high-gain antennas with circular polarization are preferable because of their ability to resist to multipath effects, polarization mismatch and weather conditions (i.e. rain or snow) [1], [2].

Various methods can be used for realizing a CP beam antenna. A first technique employs polarizers [2], [3]. If a multilayer configuration [4] is used, then a wide bandwidth can be obtained but both the losses and length of the antenna are increased because of the additional element, the polarizer. A second technique uses only one feeding port and has a compact configuration, but the downside of this technique is that, a narrow bandwidth is usually obtained [5]. A third method, called the multi-feeding technique, has two to four feeding ports that are excited with equal amplitude and 90° phase difference. A popular multi-feeding technique is the sequential parallel feeding method. It consists in using four single-feeding radiating elements that are rotated clockwise or anticlockwise resulting in an improved axial ratio (AR) bandwidth with minimum losses [7].

In [7] a 2×2 CP microstrip antenna array that operates in Ka-band is presented. The antenna shows a maximum measured gain of 13.59 dBi at 29.3 GHz and an axial ratio lower than 3 dB in between 28.4 GHz and 30 GHz. Still, the authors do not give any insight into how to switch the main beam direction of radiation. In [8] a 60 GHz CP antenna array for line-of-sight train-to-train communications is proposed. The antenna shows high directivity and a wide bandwidth from 55.1 GHz to 60.5 GHz. The disadvantage of this antenna is that it has a thickness of 792 μm which makes it difficult to integrate in certain devices. A planar CP

The associate editor coordinating the review of this manuscript and approving it for publication was Jaime Laviada.

substrate integrated waveguide (SIW) stacked patch antenna array that consists of four sequential-rotation (SR) subarrays in Ka-band is presented in [9]. The antenna demonstrates a 20.32 dBi gain, a working bandwidth of 29.6% and an AR bandwidth of 25.4%. The downside of this antenna is that it is very difficult to realize and it only radiates in the broadside direction.

Tilting the beam of an antenna can be achieved by using electronic or mechanic devices. These types of antennas are capable of changing their main direction of radiation and they can represent a highly attractive solution for 5G wireless networks. Electronic devices use active elements like PIN/varactor diodes and RF MEMS switches [10] that result in gain dropping when the beam is tilted. Mechanical devices conserve the gain and can obtain a wider scan angle. More recently, periodic structures (high impedance surfaces, frequency selective surface (FSS) [11], electromagnetic band gap (EBG) [12], artificial magnetic conductor (AMC) [13] and split ring resonators [14]) have started to play a key role for obtaining a tilted beam antenna because they exhibit bandpass and bandstop properties, they are easy to fabricate and they are low cost. Sievenpiper *et al.* [15] have presented a tunable impedance surface with vias that use multiple varactor diodes and can obtain a beam steering of $\pm 40^\circ$ at 4.5 GHz. Dadgarpour *et al.* [14] have proposed a 5×4 double G-shaped resonator array that works in H-plane for tilting the beam of a bow-tie antenna at 3.5 GHz by $\pm 32^\circ$. However, the proposed approach uses a multilayer structure that can increase the complexity of the antenna and the cost. In [16], a single layer FSS structure with double configuration has been placed under the directors of a Yagi-Uda antenna for obtaining a measured beam-tilting from $+23^\circ$ to -29° in the end-fire direction at 30 GHz. Mantash *et al.* [17] have proposed a flexible reconfigurable pattern antenna using an AMC in Ka-band. The AMC-antenna exhibits five beam-tilting angles in H-plane with a gain of 12.1 dBi at 29.5 GHz. It was also demonstrated that by using a SPDT switch, the main beam can be electronically tilted in the elevation plane from $+32^\circ$ to -23°. Furthermore, in Table 1 the performances of various beam steering antennas proposed in literature are shown in comparison with the antenna proposed in this study.

To change the direction of the radiation pattern from end-fire to full broadside, a new technique based on using an EBG structure is proposed in this paper. The EBG structure is placed around a CP antenna in order to provide beam-switching capabilities. This resulted in a high beam tilting angle, of $+90^\circ$. To the best of our knowledge, the beam tilting angle obtained here is three times higher than all known proposals presented in Table 1. This approach allows the antenna array direction of radiation to be dynamically controlled. When the system is used without EBG, then the circularly polarized wave, obtained by employing the sequential feeding, is directed into the end-fire horizontal plane (0°). At the same time, by using a mechanical device, the EBG can be placed around the antenna, resulting in a beam tilting

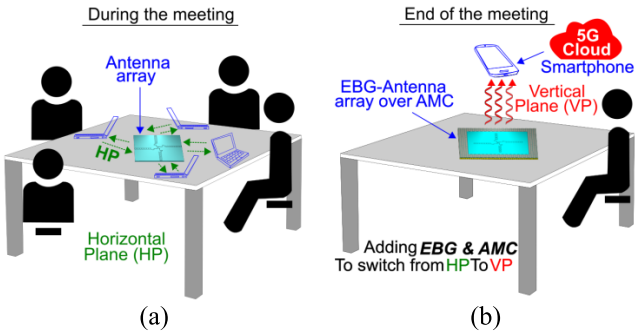

FIGURE 1. Antenna usage scenarios: (a) conference meeting, (b) cloud transfer.

of 90°, with better performance (gain and axial ratio band enhancement). This innovative, refined and effective approach can give to the antenna multiple uses. A possible antenna usage scenario is represented in Fig. 1.

Fig. 1(a) presents a scenario where during a meeting the synchronization between the computers of four users is needed. In this case, the antenna array, without EBG, can be used for transmitting/receiving data. Moreover, after the meeting has ended, a Cloud transfer or Cloud synchronization (5G communication) can be performed. The user can place his smartphone over the AMC-antenna, with EBG in this case (see Fig. 1(b)), and the transfer of the saved data can easily begin. By only taking this example, the novel antenna could be used to facilitate and decrease the time needed in a meeting. Indubitably, other usage scenarios for this antenna array can be envisioned for 5G communication networks. The steps pursued for realizing the antenna array are explained in Fig. 2.

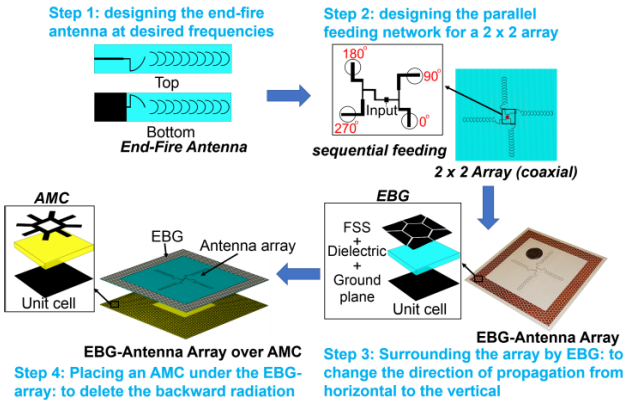

FIGURE 2. Realization process of the proposed EBG-AMC-antenna array.

The article is structured as follows: in Section II the various elements that form the antenna array are studied, including the periodic structures involved in the realization. In Section III, the design procedure is explained step by step. Section IV presents the experimental results that validate the proposed antenna, and Section V concludes that paper.

TABLE 1. Comparison of proposed antenna with reference antennas.

Ref.	Size [mm]	Realization technique	CP technique feeding	Beam tilting technique	Beam tilting angle [°]	BW [GHz]	AR BW [GHz]	Realized gain [dBi]	Cost	Realization
[1]	72x48x2.2	PCB process	Single	No beam tilting	-	26.5-40	26.4-30.3	17.4-18.2	Low	Easy
[2]	120x120x1.681	Etching	Sequential	No beam tilting	-	24-34	24-31	16.29	Low	Easy
[18]	18.6x60 x0.127	Etching	No CP	Radiating elements ⊥ to feeding line	+30°	76.5	-	-	Low	Medium
[19]	30x30x31	Mechanical	Circular horn antennas	Dielectric lens	±45°	57-66	57 -66	13.3-14.4	High	Hard
[20]	25x25x9.6	PCB process	No CP	Quartz lens	±35°	52-68.9	-	8.46	High	Hard
[21]	218x53x73	Etching	No CP	EBG	+25°	3.5	-	4.7	Low	Medium
[22]	60x40x1.575	Etching	No CP	Metamaterial	+17°	7.3-7.5	-	8.7-9.25	Low	Easy
[23]	11.1x7.4x2.674	Etching	No CP	HRIM	+30°	57-64	-	10.5-12	Low	Medium
Proposed antenna	140x140x3.754	Etching	Sequential	EBG	0° – 90°	26.5-31.5	28-31	10.2-11.9	Low	Easy

II. DESIGN OF THE ANTENNA ARRAY AND PERIODIC STRUCTURES

A. END-FIRE ANTENNA

Classical Yagi antennas are based on metallic bars from which the directions, reflectors and half-wavelength dipole are realized. The half-wavelength dipole is directly fed by a transmission line while the directors/reflectors act as parasitic radiators whose currents are obtained by mutual coupling. The parasitic elements in the front of the half-wavelength dipole act as directors while in the rear they act as reflectors. In order to obtain an end-fire beam the directors are smaller in length than the dipole. More recently, printed Yagi antennas were developed. These antennas are widely used because they are low-cost, low-profile, highly versatile and have high efficiency.

The antenna chosen for this study is an end-fire Yagi-Uda antenna, presented in Fig. 3, which has microstrip feeding. It is essentially made of a driven dipole and 10 semicircles, with an overall size of 39 mm × 10 mm (Length × width) and is printed on a Rogers RO3006 substrate with permittivity of $\varepsilon_r = 6.15$ and thickness of h = 0.254 mm.

The 3D simulated radiation pattern of the single element antenna at 29.25 GHz is shown in Fig. 3(b). The directive beam is oriented in the end-fire direction with a maximum gain of 6.89 dBi.

The principle of operation for this antenna (Fig. 3(c)) is no different than the one for the classical Yagi-Uda antenna explained above with the only difference that the driven dipole and semicircles are printed on both sides of the substrate. This allows for a wider balun feed from the microstrip-line to the driven dipole. Furthermore, the truncated ground plane acts as a reflector.

In Fig. 4, the simulated reflection coefficient of the single element antenna including the connector is shown and from the results obtained the single element resonates at 30 GHz

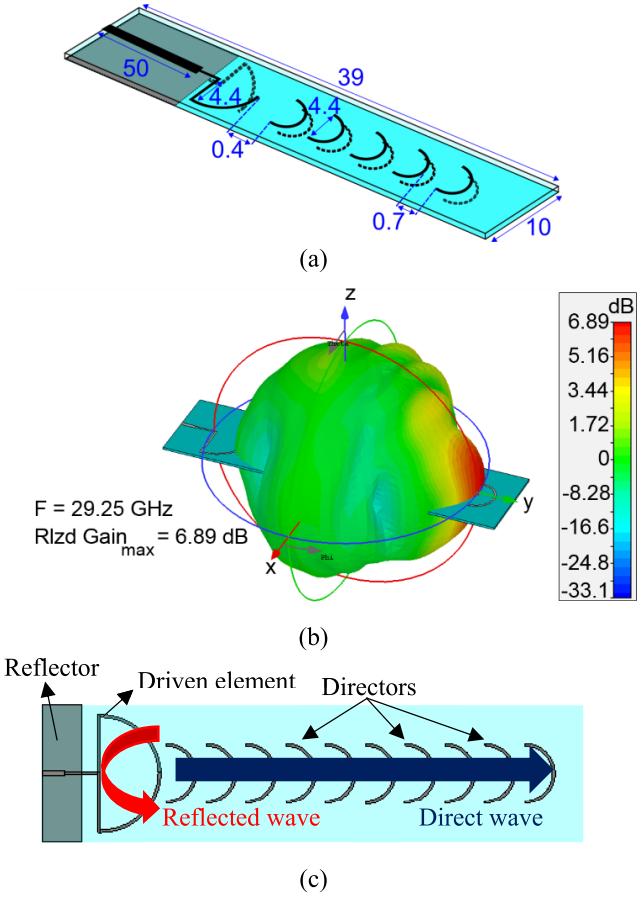

FIGURE 3. Design of: (a) the proposed Yagi-Uda antenna (dimensions are in mm), (b) 3D radiation pattern at 29.25 GHz and (c) operational principle of the Yagi-Uda antenna.

and covers the frequency band (29 GHz – 31.4 GHz) with a maximum realized gain of 6.89 dBi at 29.25 GHz. It can also be observed that an increase of 130% in bandwidth is

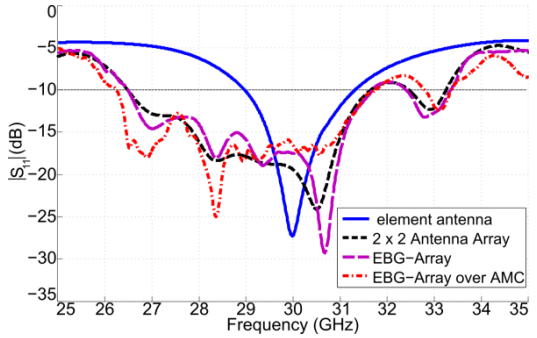

FIGURE 4. Simulated reflection coefficient of all antenna configurations.

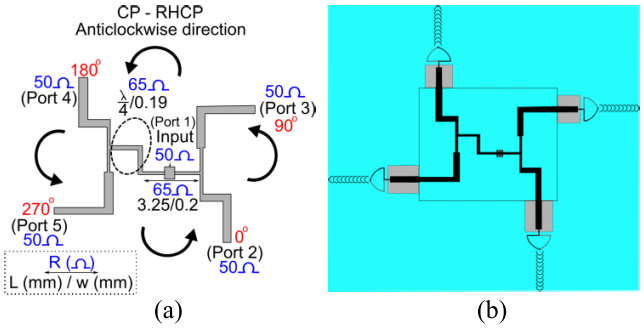

FIGURE 5. Design of: (a) parallel feeding network and (b) 2 × 2 antenna array with the feeding network.

obtained when the 2 × 2 antenna array with EBG and AMC is used.

B. SEQUENTIAL FEEDING AND ARRAY DESIGN

The feeding network used here will convert the linearly polarized antenna into a circularly polarized beam antenna. In Fig. 5(a) all the parameter values for realizing the feed, carefully optimized to obtain a sequential feeding at 30 GHz, are shown. The feeding network is based on the models presented in [2] and [24]. In this work, one novelty consists in the fact that the array is fed by a coaxial feed in one location while the models presented in [2] and [24] are based on microstrip line feeding. This novel approach minimizes the antenna length and the cost without any decrease in performance. The network is composed of two T-junction sections, which include an anti-phase feeding network and two 90° phase difference feeding portions. The Input (Port 1), seen in Fig. 5(a), is an anti-phase equal power divider that gives an 180° phase difference in between the output ports. To obtain a 90° phase difference for each output of the feeding network, each output of the anti-phase divider is connected to another power divider. The 50 ohms impedance obtained at the output of each port depends on the length and width of each T-junction.

The simulated S-parameters of the isolated parallel feeding network are presented in Fig. 6. The S(1,1) is lower than –15 dB in the frequency band 25 to 35 GHz (Fig. 6(a)). Each output port has an almost 90° phase difference from the other ports in the studied frequency band (Fig. 6(b)).

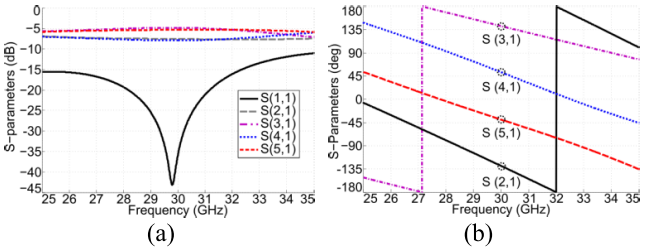

FIGURE 6. Simulated S-parameters of the parallel feeding network: (a) amplitude and (b) phase.

The 2 × 2 antenna array with the feeding network will then be printed on the Rogers RO3006 substrate, as shown in Fig. 5(b). The corresponding CST Microwave Studio simulation results are presented in Fig. 4. The simulated reflection coefficient in dB shows that the novel antenna array has an increased bandwidth (26.5 to 31.61 GHz), and a maximum realized gain of 9.33 dBi at 29 GHz. By comparing the reflection coefficient results of the single element Yagi-Uda antenna with the antenna array, a very good increase in bandwidth, of 130%, is obtained for the array. The simulated realized antenna array gain and total efficiency are represented in Fig. 7. We have calculated the total efficiency by determining the ratio in between the radiated power to the input power of the antenna and then multiplied the result with the antenna's loss due to impedance mismatch. The 2 × 2 antenna array has a gain that ranges from 8.3 dBi to 9.33 dBi and a good total efficiency of 94.3%–94.6%.

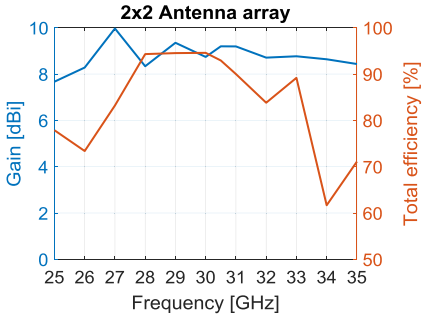

FIGURE 7. Gain and total efficiency of the 2 × 2 antenna array with parallel feeding network.

C. ELECTROMAGNETIC BAND GAP UNIT-CELL

The design of the chosen unit-cell is represented in Fig. 8(a). In this article, an EBG structure that works in the 28 – 32 GHz band is developed. The proposed structure has a hive shaped form. The length of the hexagon unit cell is of 2 mm and the periodicity of 0.3 mm. In Fig. 8(b), the simulated transmission coefficient of the 2 × 3 EBG structure is shown. From the obtained results, a transmission coefficient lower than −10 dB is achieved in the band between 28 GHz to 32 GHz, making the unit-cell ideal for our purposes. This means that in this frequency band, the electromagnetic wave will not propagate resulting in beam tilting of the antenna array.

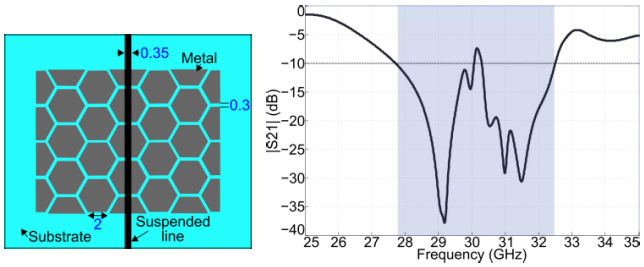

FIGURE 8. Design of: (a) proposed EBG structure with suspended strip line and (b) simulated transmission coefficient of the suspended line above the 2 × 3 EBG structure.

D. AMC UNIT-CELL

A plentiful number of research articles have had as sole focus the replacement of the perfect electric conductor (PEC) reflector plane for low-profile antennas as a means of increasing the antenna performance [13]. This is why, in this article, an AMC is associated to the antenna, to reduce the backward radiation and also to increase the performance of the antenna array regarding the gain, the quality factor and the bandwidth.

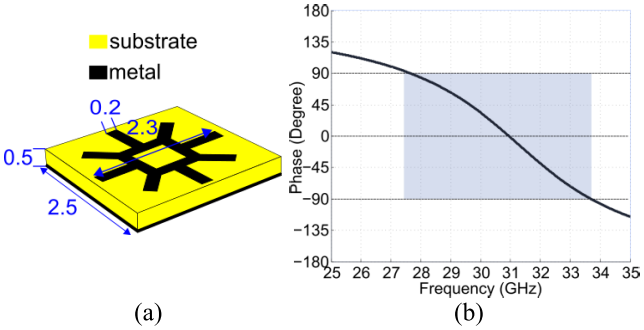

FIGURE 9. Design of: (a) proposed AMC unit-cell and (b) reflection phase of the AMC structure.

A square loop AMC with 8 strip lines placed in a circularly form around the square is used. The proposed AMC design is shown in Fig. 9(a). One AMC unit-cell has the size of 2.5 mm × 2.5 mm, the periodicity of 0.4 mm and is printed on a Rogers RO4003C substrate with the permittivity of $\varepsilon_r = 3.38$ and the thickness of h = 0.508 mm.

An AMC is defined in the frequency band where the phase of the reflection coefficient is between −90° and 90°, or more exactly, in the frequency band where interference occurs in between the incident and reflected waves. Floquet theory was considered in CST Microwave Studio for simulating the AMC. From the results shown in Fig. 9(b), the AMC works in the 28 – 33 GHz frequency band. The unit-cell AMC is then arranged in a 140 mm × 140 mm array to form the AMC array that will be placed under the antenna to reduce the backward radiation.

III. EBG-AMC-ANTENNA ARRAY DESIGN

The approach chosen for realizing the antenna is shown in Fig. 10. The total size of the antenna that includes the sequential feeding and EBG structure, is 140 mm × 140 mm.

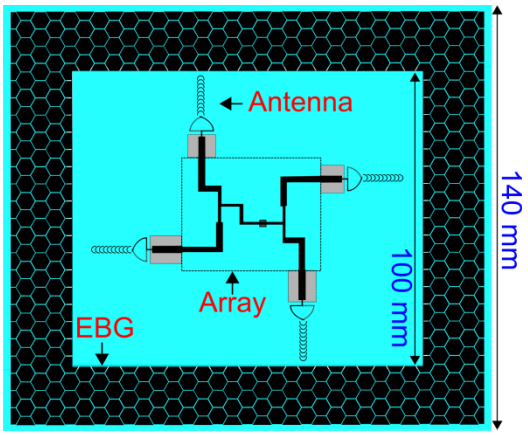

FIGURE 10. Proposed EBG-antenna array.

Compared with the antenna element, the refection coefficient of the EBG-antenna array, represented in Fig. 4, shows a 130% increase in bandwidth. Because the EBG works in the same frequency band as the antenna array then its impact over the S_{11} of the antenna will be negligible. The goal is to change the direction of the end-fire radiation without diminishing the performance of the antenna by using the EBG structure.

Since the EBG structure presents a stop band in the same frequency band where the 2 × 2 antenna array works, then the beam will be deflected from the azimuth plane to the elevation plane, resulting in a beam tilting angle of 90° and an increase in performance. Thus, a beam switching system can be realized, depending on the needs of the user and the application.

The antenna array does not have a ground plane so the radiation will propagate in the ±z plane. Furthermore, by leaving the EBG-antenna array without ground plane could decrease the total performance of the antenna.

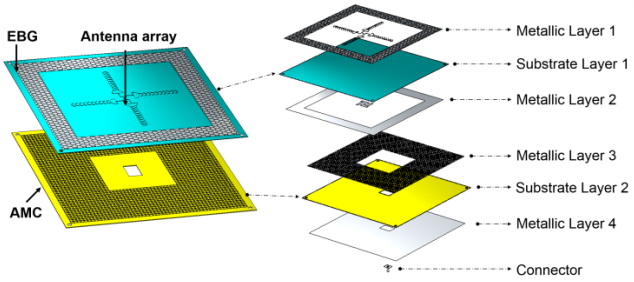

FIGURE 11. Final design of the EBG-Antenna array on AMC.

The solution proposed in this paper, for prohibiting the backward radiation from propagating is to use an AMC structure. The final design of the EBG-antenna array with AMC is shown in Fig. 11. As it can be observed, the AMC array has the same dimensions as the antenna array and is placed 3 mm underneath the antenna. A crucial aspect, that has to be taken into account, is the mutual coupling between the antenna and the AMC plane. If the coupling is extremely strong, that this will greatly affect the antenna array performance. To prevent this behavior, the AMC array is changed as follows: the unit

cells from the center region of the AMC plate that are located exactly underneath the feeding network of the antenna array are removed. The gap where no AMCs can be found has the dimensions of 50 mm × 50 mm. Also, a small slot is cut in the AMC substrate to accommodate the connector.

TABLE 2. Effect of AMC and EBG on the 2 × 2 antenna-array performance.

Config.	Units	Single element antenna		Antenna array		EBG Antenna array		EBG AMC Antenna array	
Frequency	GHz	29	30	29	30	29	30	29	30
Total efficiency	%	89	99.6	94.5	94.6	91.4	89.8	85	81.7
Simulated Realized Gain	dBi	6.8	5.8	9.3	8.72	10.6	10.8	11.9	10.2
Measured Realized Gain	dBi	-		-		-		11.2	9.55
AR bandwidth	GHz	-		28.8-30.3		28.9-30.5		28.0-31.0	
Bandwidth	GHz	29.0-31.4		26.5-31.6		26.5-31.7		26.2-31.7	

In Table 2 the performances of all antenna configurations are shown and compared. From the results, it can be distinguished that by adding the sequential feeding network and designing the antenna array, the simulated realized gain increased from 6.8 dBi to 9.3 dBi at 29 GHz. An average gain improvement of 2.5 dBi is obtained at the studied frequencies when the antenna array is employed. At the same time, the simulated realized gain of the antenna array, with EBG in this case, increased by 1.3 dBi and 2 dBi at 29 GHz and 30 GHz, respectively.

A very good gain percentage increase, of 36%, compared to the single element antenna is obtained. In addition, when the AMC structure is added, the simulated realized gain increased again by 1.3 dBi at 29 GHz, and remained constant at 30 GHz by comparison with the EBG-antenna array. A good agreement is obtained between the simulated and measured realized gain for the final structure (EBG-antenna array over AMC).

In terms of AR bandwidth, it can be clearly seen that it remains almost constant when the EBG and AMC are added to the antenna array, from 28 to 31 GHz.

The single element antenna presents a working bandwidth of 2.4 GHz, the antenna array of 5.11 GHz, the EBG-antenna array of 5.2 GHz and the final EBG-AMC-antenna array of 5.5 GHz. A more than 130% increase in bandwidth is obtained for the final structure compared to the single element Yagi-Uda antenna. In conclusion, the working antenna bandwidth increased exponentially with each element added.

To validate the proposed antenna design, the 3D radiation patterns of the different antenna configurations, were simulated using CST Microwave Studio, and are depicted in Fig. 12. The objective of this research is to design a structure that offers beam steering capabilities. From Fig. 12(a) it

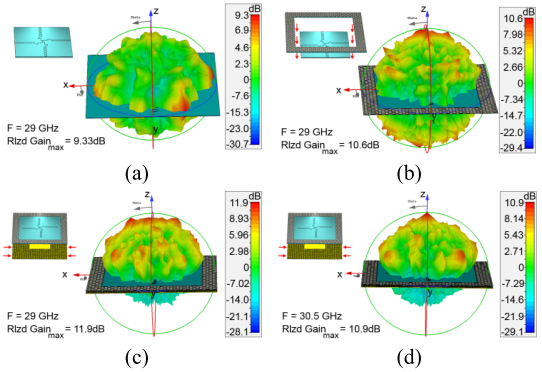

FIGURE 12. 3D simulated radiation pattern for the 2 × 2 antenna array at 29 GHz with: (a) sequential feeding network, (b) EBG interconnection, (c) EBG - AMC and (d) EBG – AMC at 30.5 GHz.

can be seen that when the 2 × 2 antenna array using the multi-feeding method is simulated, a realized gain of 9.33 GHz is obtained at 29 GHz and the maximum radiation is directed in the end-fire direction. When the EBG periodic structure is placed around the antenna, the maximum radiation is directed into the broadside direction (±z plane), as it is shown in Fig. 12(b). The realized gain also increased by 12%, arriving to 10.6 dBi at 29 GHz. Furthermore, by placing the AMC underneath the antenna, the backscattered wave is minimized and, at the same time, the gain augmented again, reaching 11.9 dBi at the same frequency. This means a gain increases of 21.6% and of 11% compared to the antenna array alone and with the EBG-antenna array configurations. The 3D radiation pattern of the EBG-antenna array over AMC at 30.5 GHz is also shown in Fig. 12(d). A maximum realized gain of 10.9 dBi is reached. Moreover, it can be observed that, at 30 GHz, the radiation pattern has a more uniform and directive shape than at 29 GHz. This can be explained by the fact that the EBG and AMC have been optimized to work especially at 30 GHz.

IV. EXPERIMENTAL RESULTS

To justify and validate the proposed final antenna (EBG-antenna array on AMC), a prototype was fabricated and shown in Fig. 13. Here, to avoid getting mechanical flaws, the EBG was printed directly on the same substrate of the array. It means the antenna substrate is expanded. Another prototype could be realized only for the EBG structure that will take place the antenna around using a mechanical technique. An AMC (Fig. 13(c)), was fabricated and placed 3 mm underneath the EBG-array. Four thru were realized in the four corners of the structure so that the AMC can be then screwed to the back of the antenna by using plastic bolts. A 2.92 mm (K) connector is placed on the back of the EBG antenna array just like it is laid out in Fig. 13(b). The final simple and elegant design, with the dimensions 140 mm × 140 mm, is displayed in Fig. 13(d).

The simulated and measured reflection coefficients of the EBG-antenna array on AMC are presented in Fig. 14(a). The measured magnitude of the reflection coefficient is obtained

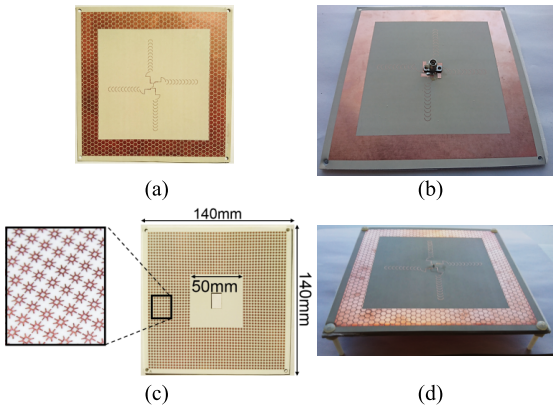

FIGURE 13. Design of: (a) top view of the array, (b) back view of the array, (c) AMC plate and (d) realized EBG-antenna array on AMC.

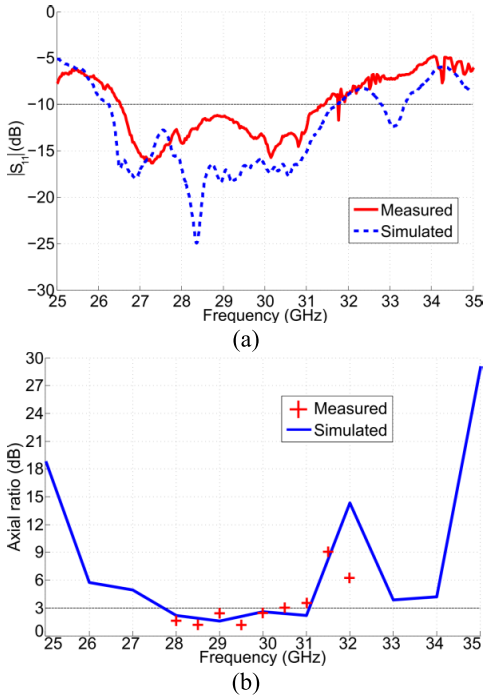

FIGURE 14. Simulated and measured: (a) reflection coefficient and (b) axial ratio results of the EBG-antenna array over AMC.

by using an Anritsu M54647A 70 GHz vector network analyzer. A good agreement is obtained between the simulation and measurement results. It can be noticed that in between 26.2 GHz and 31.7 GHz the reflection coefficient is lower than −10 dB, confirming that the antenna works in the desired frequency band. The final bandwidth of the antenna is of 5.5 GHz. It can also be seen that the measured resonant frequency shifted slightly to higher frequencies and this can be attributed to the fabrication tolerance of the antenna elements (permittivity of the substrate) and the presence of the connector.

The axial ratio of the final EBG-array over AMC is also simulated and measured and it is shown in Fig. 14(b). The antenna exhibits a 3 dB axial ratio bandwidth from 28 to 31 GHz with a fractional bandwidth of 10.17%. This indicates that in the desired frequency band, the antenna has circular polarization, especially at 30 GHz where the AR became 2.9 dB.

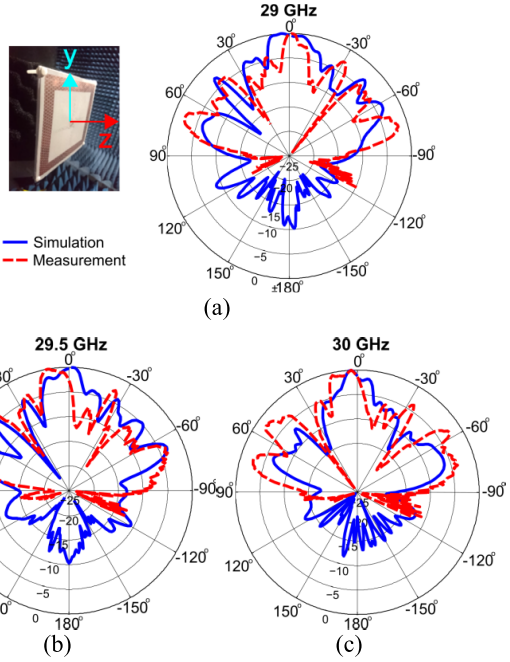

FIGURE 15. Representation of: (a) normalized H-plane measured and simulated radiation patterns of the antenna array system at: (a) 29 GHz, (b) 29.5 GHz and (c) 30 GHz.

The peak realized antenna gain and radiation patterns of the proposed antenna are measured in a MM-wave anechoic chamber using the gain comparison approach. This technique entails that the received power of a reference antenna and prototype antenna is measured and the gain is determined by taking into account the difference in between the two received powers. The simulated and measured normalized radiation patterns at three frequencies, in the H-plane (broadside) are shown in Fig. 15.

From Fig. 15 it can be observed that the measurement is in good agreement with the simulation for all studied frequencies and that the backscattered wave is minimal. In addition, the maximum measured realized peak gain was found to be 11.2 dBi, when employing the AMC at 29 GHz.

V. CONCLUSION

A novel circularly polarized EBG-array antenna on AMC has been presented in this paper. The proposed antenna provides a full beam tilting from 0° to 90° with CP capabilities, it is low cost and it can be easily manufactured, as opposed to literature antennas that either have no CP, have low tilting angle or are very difficult to realize. The single element antenna used to realize the design is a Yagi-Uda antenna. For obtaining a circularly polarized beam, a sequential feeding network with four output ports having 90° phase delays placed in an anti-clock-wise sequence is necessary. Here, as

opposed to using a microstrip line for alimenting the antenna, a coaxial feeding in one location has been proposed. This technique simplifies and minimizes the design.

The proposed approach consists in placing an EBG around the antenna array, giving it a good beam switching functionality. A full beam tilting from the end-fire direction to the broadside direction is observed, resulting in a beam switching from 0° to 90°. An AMC has also been placed under the antenna to stop the backward radiation and increase the performance.

Proof-of-concept was demonstrated in the possible 5G frequency band (28 – 31 GHz). A measured working bandwidth of 5.5 GHz, realized gain of 11.2 dBi and an AR equal to 2.9 dB have been obtained for the final antenna design. In conclusion, this antenna array can represent a nice solution for future 5G applications.

REFERENCES

[1] J. Wu, Y. J. Cheng, and Y. Fan, "Millimeter-wave wideband high-efficiency circularly polarized planar array antenna," *IEEE Trans. Antennas Propag.*, vol. 64, no. 2, pp. 535–542, Feb. 2016.

[2] M. Akbari, S. Gupta, M. Farahani, A. R. Sebak, and T. A. Denidni, "Analytic study on CP enhancement of millimeter wave DR and patch subarray antennas," *Int. J. RF Microw. Comput.-Aided Eng.*, vol. 27, no. 1, Jan. 2017, Art. no. e21053.

[3] M. Mantash, M. B. Kakhki, and T. A. Denidni, "Millimeter-wave circularly polarized Vivaldi antenna using simple single layer 2D FSS polarizer," in *Proc. 18th Int. Symp. Antenna Technol. Appl. Electromagn.*, Aug. 2018, pp. 1–2.

[4] M.-A. Joyal and J.-J. Laurin, "Analysis and design of thin circular polarizers based on meander lines," *IEEE Trans. Antennas Propag.*, vol. 60, no. 6, pp. 3007–3011, Jun. 2012.

[5] K. F. Tong and T. P. Wong, "Circularly polarized U-slot antenna," *IEEE Trans. Antennas Propag.*, vol. 55, no. 8, pp. 2382–2385, Aug. 2007.

[6] Y.-X. Guo, K.-W. Khoo, and L. C. Ong, "Wideband circularly polarized patch antenna using broadband baluns," *IEEE Trans. Antennas Propag.*, vol. 56, no. 2, pp. 319–326, Feb. 2008.

[7] A. Chen, Y. Zhang, Z. Chen, and S. Cao, "A Ka-band high-gain circularly polarized microstrip antenna array," *IEEE Antennas Wireless Propag. Lett.*, vol. 9, pp. 1115–1118, Dec. 2010.

[8] A. Al-Bassam, W. Alshrafi, and D. Heberling, "A 60 GHz circularly polarized antenna array for line-of-sight train-to-train communication," in *Proc. 11th German Microw. Conf. (GeMiC)*, Mar. 2018, pp. 148–151.

[9] H. Xu, J. Zhou, K. Zhou, Q. Wu, Z. Yu, and W. Hong, "Planar wideband circularly polarized cavity-backed stacked patch antenna array for millimeter-wave applications," *IEEE Trans. Antennas Propag.*, vol. 66, no. 10, pp. 5170–5179, Oct. 2018.

[10] M. Sazegar *et al.*, "Beam steering transmitarray using tunable frequency selective surface with integrated ferroelectric varactors," *IEEE Trans. Antennas Propag.*, vol. 60, no. 12, pp. 5690–5699, Dec. 2012.

[11] B. A. Munk, *Frequency Selective Surfaces: Theory and Design*. New York, NY, USA: Wiley, 2000.

[12] F. Yang and Y. Rahmat-Samii, *Electromagnetic Band Gap Structures in Antenna Engineering*. Cambridge, U.K.: Cambridge Univ. Press, 2009.

[13] M. Mantash and A.-C. Tarot, "On the bandwidth and geometry of dual-band AMC structures," in *Proc. 10th Eur. Conf. Antennas Propag. (EuCAP)*, Davos, Switzerland, Apr. 2016, pp. 1–4.

[14] A. Dadgarpour, B. Zarghooni, B. S. Virdee, and T. A. Denidni, "Enhancement of tilted beam in elevation plane for planar end-fire antennas using artificial dielectric medium," *IEEE Trans. Antennas Propag.*, vol. 63, no. 10, pp. 4540–4545, Oct. 2015.

[15] D. F. Sievenpiper, J. H. Schaffner, H. J. Song, R. Y. Loo and G. Tangonan, "Two-dimensional beam steering using an electrically tunable impedance surface," *IEEE Trans. Antennas Propag.*, vol. 51, no. 10, pp. 2713–2722, Oct. 2003.

[16] M. Mantash, A. Kesavan, and T. A. Denidni, "Beam-tilting endfire antenna using a single-layer FSS for 5G communication networks," *IEEE Antennas Wireless Propag. Lett.*, vol. 17, no. 1, pp. 29–33, Jan. 2018.

[17] M. Mantash, A. Kesavan, and T. A. Denidni, "Millimetre-wave antenna with tilted beam for future base station applications," *IET Microw., Antennas Propag.*, vol. 13, no. 2, pp. 223–230, 2018.

[18] Y. Kashino, K. Sakakibara, Y. Tanaka, N. Kikuma, and H. Hirayama, "Design of millimeter-wave microstrip comb-line antenna array beam-tilting in perpendicular plane of feeding line," in *Proc. Asia–Pacific Microw. Conf.*, Dec. 2006, pp. 817–820.

[19] J. R. Costa, E. B. Lima, and C. A. Fernandes, "Compact beam-steerable lens antenna for 60-GHz wireless communications," *IEEE Trans. Antennas Propag.*, vol. 57, no. 10, pp. 2926–2933, Oct. 2009.

[20] A. Artemenko, A. Maltsev, R. Maslennikov, A. Sevastyanov, and V. Ssorin, "Beam steerable quartz integrated lens antenna for 60 GHz frequency band," in *Proc. Eur. Conf. Antennas Propag.*, Apr. 2011, pp. 758–762.

[21] I. Kim and Y. Rahmat-Samii, "Beam-tilted dipole-EBG array antenna for future base station applications," in *Proc. IEEE Antennas Propag. Soc. Int. Symp.*, Jul. 2013, pp. 1224–1225.

[22] A. Dadgarpour, B. Zarghooni, B. S. Virdee, and T. A. Denidni, "Beam tilting antenna using integrated metamaterial loading," *IEEE Trans. Antennas Propag.*, vol. 62, no. 5, pp. 2874–2879, May 2014.

[23] A. Dadgarpour, B. Zarghooni, B. S. Virdee, and T. A. Denidni, "Improvement of gain and elevation tilt angle using metamaterial loading for millimeter-wave applications," *IEEE Antennas Wireless Propag. Lett.*, vol. 15, pp. 418–420, 2015.

[24] S. L. S. Yang, R. Chair, A. A. Kishk, K. F. Lee, and K. M. Luk, "Study on sequential feeding networks for subarrays of circularly polarized elliptical dielectric resonator antenna," *IEEE Trans. Antennas Propag.*, vol. 55, no. 2, pp. 321–333, Feb. 2007.

MOHAMAD MANTASH (SM'18) received the master's degree in electronics and microwave systems from Pierre and Marie Curie University—Paris VI, France, in 2010, and the Ph.D. degree in signal processing and telecommunications from the University of Rennes 1, Rennes, France, in 2013.

From 2013 to 2014, he was a Telecommunications Engineer with AFD Technologies, Paris, France, and from 2014 to 2016, he was a Research Engineer with the Antennas and Microwaves Group, Institute of Electronic and Telecommunications of Rennes, Rennes, France. He is currently a Postdoctoral Fellow with the Institut National de la Recherche Scientifique, University of Quebec, Montreal, QC, Canada. His current research interests include metamaterials, such as frequency-selective surfaces, electromagnetic bandgaps, and artificial magnetic conductors for beamforming applications, reconfigurable antennas, and the design and development of wearable antennas and array antennas at microwave and millimeter-wave frequencies.

TAYEB A. DENIDNI (SM'04–F'19) received the M.Sc. and Ph.D. degrees in electrical engineering from Laval University, Quebec, QC, Canada, in 1990 and 1994, respectively.

From 1994 to 2000, he was a Professor with the Engineering Department, University of Quebec at Rimouski, Rimouski, QC, Canada, where he founded the Telecommunications Laboratory. Since 2000, he has been with the Institut National de la Recherche Scientifique (INRS), University of Quebec, Montreal, QC, Canada. He founded the RF Laboratory, INRS-Energie, Materiaux et Telecommunications (INRS-EMT), Montreal. He has extensive experience in antenna design. He leads a large research group consisting of three research scientists, six Ph.D. students, and one M.Sc. student. He served as a Principal Investigator on many research projects sponsored by NSERC, FCI, and numerous industries. His current research areas of interest include reconfigurable antennas using electromagnetic bandgap and frequency-selective surface structures, dielectric resonator antennas, metamaterial antennas, adaptive arrays, switched multi-beam antenna arrays, ultrawideband antennas, microwave, and development for wireless communications systems.